Palaeogeography, Palaeoclimatology, Palaeoecology 490 (2018) 227–239

Contents lists available at ScienceDirect

Palaeogeography, Palaeoclimatology, Palaeoecology

journal homepage: www.elsevier.com/locate/palaeo

Provenance, sea-level and monsoon climate controls on silicate weathering of Yellow River sediment in the northern Okinawa Trough during late last glaciation

Debo Zhao[a,c], Shiming Wan[a,b,*], Peter D. Clift[d], Ryuji Tada[e], Jie Huang[a], Xuebo Yin[a], Renqiang Liao[a], Xingyan Shen[a], Xuefa Shi[b,f], Anchun Li[a]

[a] Key Laboratory of Marine Geology and Environment, Institute of Oceanology, Chinese Academy of Sciences, Qingdao 266071, China
[b] Laboratory for Marine Geology, Qingdao National Laboratory for Marine Science and Technology, Qingdao 266061, China
[c] University of Chinese Academy of Sciences, Beijing 100049, China
[d] Department of Geology and Geophysics, Louisiana State University, Baton Rouge, LA 70803, USA
[e] Department of Earth and Planetary Science, University of Tokyo, Tokyo 113-0033, Japan
[f] Key Laboratory of Marine Sedimentology and Environmental Geology, First Institute of Oceanography, SOA, Qingdao 266061, China

ARTICLE INFO

Keywords:
Sediment provenance
Climate change
Northern Okinawa Trough
East China Sea
Elements geochemistry
Clay minerals

ABSTRACT

High resolution multi-proxy records, including geochemical and grain-size data from detrital sediments of IODP Site U1429 in the northern Okinawa Trough, provide reliable evidence for constraining sediment source and transport processes. They also allow silicate weathering and erosion controlled by sea-level change and East Asian summer monsoon evolution since 34 ka to be reconstructed. Provenance proxies indicated that sediments in the northern Okinawa Trough were mainly supplied by the Yellow River middle reach at ~34–8 ka. The low sea level and proximity of paleo-Yellow River mouth to the northern Okinawa Trough were the causes of the dominant Yellow River input. After ~8 ka, a retreated Yellow River mouth coupled with the blocking effect of the Kuroshio Current and its branches, together with strong East Asian summer monsoon precipitation resulted in relatively strong sediment input from Kyushu to the northern Okinawa Trough. Meanwhile, Yellow River upper reach supplied more sediments to the study site than that during the ~34–8 ka. On glacial-interglacial scale, silicate weathering proxies indicate that the core sediment was more weathered during the last glacial and deglacial than that in the modern Yellow River. We attribute this to the increased upper reach sediment input, which supplied more weak weathered sediment to the study site during the Holocene. Besides, composite effect of weathering during glacial and deglacial sediment production and additional weathering upon subaerial exposure of shelf deposits during low sea-level stage, as well as older weathered sediments reworking during sea-level rise could also account for this weathering regime. On multi-millennial scale, from ~34 to 18.5 ka, silicate weathering was mainly controlled by the East Asian summer monsoon, with a cooling and drying climate associated with weakened summer monsoon activity. This is consistent with the reduced alteration of sediments eroded from the Yellow River basin. From ~18.5 to 8 ka, strong reworking of older weathered sediments overwhelmed the East Asian summer monsoon in controlling silicate weathering, which induced a continuous increase in chemical alteration of the sediments during this period.

1. Introduction

Silicate weathering and erosion act together to generate soils and sculpt landscapes, and significantly regulate sediment transport from source to sink (Riebe et al., 2004). Continental silicate weathering also plays a critical role in global climate change by regulating atmospheric carbon dioxide concentrations on the long timescales. Increased rates of weathering lead to the drawdown of atmospheric carbon dioxide (Ludwig et al., 1999; Raymo et al., 1988; Riebe et al., 2004; Wan et al., 2017). Accordingly, if we are to quantify solid Earth-climate interactions then understanding how continental silicate weathering and erosion respond to the climate change is essential (Clift, 2006; Wan et al., 2012; West et al., 2005).

Silicate weathering and erosion in Asia linked to tectonic and monsoonal evolution may be one of the most significant processes affecting global climatic conditions during the Cenozoic (Berner and

* Corresponding author at: Key Laboratory of Marine Geology and Environment, Institute of Oceanology, Chinese Academy of Sciences, Qingdao 266071, China.
E-mail address: wanshiming@ms.qdio.ac.cn (S. Wan).

https://doi.org/10.1016/j.palaeo.2017.11.002
Received 30 May 2017; Received in revised form 13 October 2017; Accepted 1 November 2017
Available online 07 November 2017
0031-0182/ © 2017 Elsevier B.V. All rights reserved.

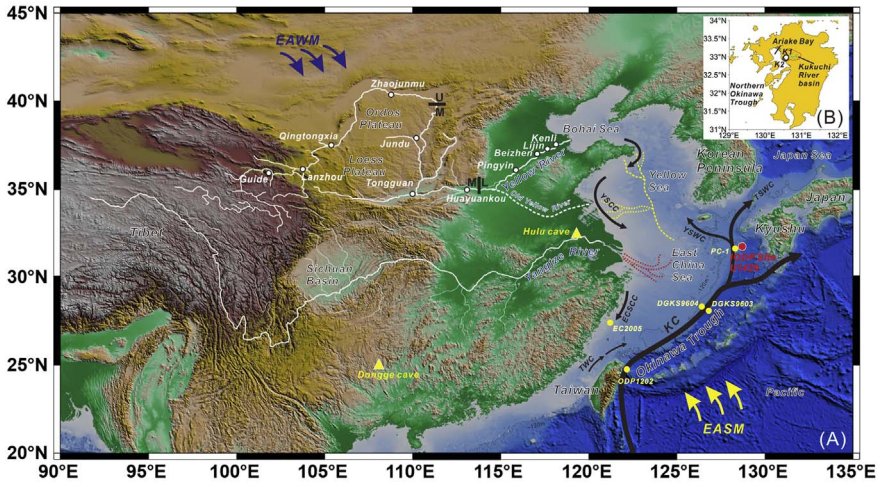

Fig. 1. (A) Locations of IODP Site U1429 and reference sites, as well as the Yellow River surface sediment samples. (B) Locations of Kyushu Kukuchi River surface sediment samples. The Yellow River drainage basin division is shown from (Nie et al., 2015). U: Upper reaches; M: Middle reaches; L: Low reaches. Old Yellow River is shown from (Liu et al., 2001). The paleo-Yellow River valleys on the Yellow Sea and north East China Sea shelves are shown in yellow dash lines which changed from (Li et al., 1991) and (Liu et al., 2010), and the paleo-Yangtze River valleys on the East China Sea shelf are shown in red dash lines changed from (Li et al., 2005). The ocean current system in East Asian marginal seas and Kuroshio Current and its branches are from (Yuan et al., 2008). The −120 m isobath is shown by gray line and approximately represents the position of the shoreline during glacial lowstands. The East Asian summer monsoon (EASM) and East Asian winter monsoon (EAWM) are shown by yellow and blue arrows, respectively. YSCC, Yellow Sea Coastal Current; YSWC, Yellow Sea Warm Current; TSWC, Tsushima Warm Current; ECSCC, East China Sea Coastal Current; KC: Kuroshio Current; TWC, Taiwan Warm Current. (For interpretation of the references to colour in this figure legend, the reader is referred to the web version of this article.)

Berner, 1997; Clift et al., 2014; Wang et al., 2003). The huge volumes of sediment eroded from Asia to its marginal seas provide us with a precious opportunity to study the interaction of continental silicate weathering and erosion with tectonic and climatic forcing processes during the Cenozoic. Such studies have been conducted based on the marine sediments around Asia over various timescales (Clift and Blusztajn, 2005; Colin et al., 2006; Dou et al., 2016; Hu, D., et al., 2012; Huang et al., 2016; Wan et al., 2015; Wei et al., 2004). Here we present a case study from the northern Okinawa Trough (Fig. 1A), where terrigenous sediments are mainly transported from East Asia to the continental shelves by great rivers (e.g., Yellow River) and/or small mountain rivers in surrounding islands. These sediments provide the opportunity to reconstruct the terrestrial silicate weathering and erosion history since the last glaciation.

The Yellow River located in the East Asia, which has a long drainage basin (5.46×10^3 km) and located in an arid, semiarid and temperate climate zone (Ju et al., 2007) with poorly developed vegetation, precipitous terrains and fragile structure of the soils in the middle-upper reaches, and relative more vegetation coverage in the lower reach (Zhang et al., 1990). Such characteristic results in the distinct chemical weathering and erosion states in different reaches, and complex river sediment sources (Hu, B., et al., 2012; Nie et al., 2015). The Yellow River delivers ~1100 million tons (Mt) of suspended sediments annually to the East Asian marginal seas (Yellow and East China Seas) (Milliman and Farnsworth, 2011). Most of the Yellow River sediments (> 95%) are thought to be trapped in the river mouth and on the East China-Yellow Sea continental shelf. Only 5% is believed to be transported further to the deep ocean (Liu et al., 2009), such as the northern Okinawa Trough (Li et al., 2015; Liu et al., 2001; Liu et al., 2010; Xu et al., 2014). It has been suggested that the mixing proportions of Yellow River sediment transported to the sea could be significantly changed by the relative sediment input from different catchments (Hu, B., et al., 2012). Therefore sediments from different reaches with different chemical weathering states transported to the sea can also account for the sediment evolution on the geological time. However, most of previous works about East Asian marginal sea sediments have paid little attention to this point.

Since the late Quaternary, the most striking oceanographic and climate changes in East Asia and its marginal seas has been sea-level fluctuation and monsoon evolution, respectively, which can strongly regulate sediment transport from continent to the marginal seas (Diekmann et al., 2008; Saito et al., 1998). During the last glacial and early deglacial period, sea level was about 80–120 m lower than today on the East China Sea shelf (Saito et al., 1998). The prominent sea-level fall led to the progradation of the coastline and exposure of the Yellow and East China Sea shelves (Li et al., 2005; Liu et al., 2010). This development favored further weathering of shelf sediments during the glacial period. As a result, large volumes of permeable shelf sediments would have been available for extended chemical weathering. On glacial-interglacial scales, sea-level change has been suggested as being a dominant factor in regulating silicate weathering flux from detrital sediments in tropical marginal seas with wide shelves (Wan et al., 2017). The subaerial exposure and weathering of unconsolidated shelf sediments during glacial sea-level lowstands resulted in enhanced silicate weathering and potentially contributed to the additional drawdown of atmospheric CO_2 during cold stages of the Quaternary (Wan et al., 2017). However, the effect of shelf weathering is unknown in mid-latitude regions, such as the south Yellow Sea and East China Sea. Besides, it has been suggested that East Asian summer monsoon precipitation would influence the chemical weathering and physical erosion in subtropical and tropical East Asia (Colin et al., 2010; Hu et al., 2013; Wan et al., 2015). However, there were still few studies from the East Asian marginal seas/northern Okinawa Trough to reveal how monsoon climate control on the Yellow River sediment chemical weathering and erosion.

Here we present a series of comprehensive, high-resolution major and trace element geochemical proxies for constraining silicate weathering and erosion. These data are coupled with high resolution grain-size data measured from Integrated Ocean Drilling Program (IODP) Site U1429 from the northern Okinawa Trough in sediments younger than 34 ka. The objectives of this study were to (1) constrain the sediment provenance and transport process in the northern Okinawa Trough since 34 ka; (2) reveal the silicate alteration state of sediments from IODP Site U1429 since the last glacial; (3) reconstruct the history of silicate weathering and erosion intensities in response to changes of monsoon climate/sea level during the late last glaciation.

2. Materials and methods

2.1. Core locations and chronological framework

IODP Site U1429 (31°37.04′N, 128°59.85′E) is located on the western continental slope of the northern Okinawa Trough in water depths of 732 m (Fig. 1A). Three holes were cored to a core composite depth below seafloor (CCSF-D) of 200 m (Tada et al., 2014). For this study, we focused on the upper 20.99 m, whose lithology is dominated by calcareous nannofossil ooze and calcareous nannofossil-rich clay. Two thick tephra layers were found at depths of 2.15–3.0 m and 17.59–18.04 m. These tephra layers are supposed to correspond to the Kikai-Akahoya (K-Ah) tephra at ~7.3 ka and Aira-Tanzawa (AT) tephra at ~26 ka commonly found in sediment cores around Japan (Chang et al., 2015; Kawahata et al., 2006; Kubota et al., 2010; Machida, 1999;

Xu et al., 2014). Besides, a thin tephra layer at depth of 5.8–5.9 m was also founded. In this study, because we only focus on discussion of silicate weathering, we exclude the geochemical and grain-size data from the tephra and turbidite layers as well as the overlying disturbed layers from further consideration.

The age model for IODP Site U1429 was built on the basis of ten accelerator mass spectrometry (AMS) ^{14}C dates, which reveals the cored sediments extend to approximately 34.04 ka, with an average sedimentation rate of about 68.5 cm/ka (Zhao et al., 2017).

In addition to the core samples, surface sediment samples were taken from the Yellow River drainage basin (upper to lower reaches: Guide, Lanzhou, Qingtongxia, Zhaojunmu, Jundu, Tongguan, Huayuankou, Pingyin, Beizhen, Lijin, Kenli) in autumn of 1983, and Kukuchi River estuary (two samples) in Kyushu Island in winter of 2016 for clay minerals and geochemical analysis (Fig. 1A and B).

2.2. Analytical methods

Geochemical analysis of major and trace element concentrations was performed on the siliciclastic sediments. A total of 418 samples from IODP Site U1429 were taken continuously at 5 cm intervals from the upper 20.99 m of the core, and 2 surface sediment samples from the Kukuchi River were taken for the major and trace element geochemical analysis. Besides, Yellow River surface sediment samples (11 samples) were taken for the trace element geochemical analysis for the source tracing. After removal of organic matter, carbonate and Fe-Mn oxides by treating with 10% H_2O_2 at 60 °C for 1 h and 0.5 N HCl at 60 °C for 2 h, respectively (Wan et al., 2010), the sediments were rinsed with deionized water three times and dried at 80 °C before grinding into powder. The pre-treated sediments were then digested by concentrated HF + HNO_3 + $HClO_4$ mixture in Teflon vessels for elemental analysis. The major and trace element concentrations were determined at the Institute of Oceanology, Chinese Academy of Sciences (IOCAS), Qingdao, using a Thermo Icap6300 ICP-AES and a Perkin-Elmer ELAN DRC II ICP-MS, respectively (Wan et al., 2015). Several USGS and Chinese rock and sediment standards (BCR-2, BHVO-2, GBW07315 and GBW07316) and blanks were repeatedly digested and analyzed in parallel with the samples to monitor the quality of ICP-MS and ICP-AES measurements. The results were generally within the range of ± 6% of the certified values. The analytical precision is generally better than 1% for major elements and 3% for trace elements.

For the grain-size analysis, the sampling depth was the same as the geochemical analysis. Samples were measured after removal of organic matter, carbonate and biogenic silica by hydrogen peroxide (15%), hydrochloric acid (0.5 mol/L) and sodium carbonate (2 mol/L), respectively (Wang et al., 2015). Grain size measurements were carried out on a Cilas 1190 L apparatus in the laboratory of IOCAS. Cilas Particle Size Analyzers account for grains in the 0.04 to 2500 μm range. The measurement repeatability of the instrument is 0.5%, and the reproducibility is better than 2%.

Clay mineral studies were carried out on the < 2 μm fraction, which was separated based on the Stoke's settling velocity principle and recovered by centrifuging (Dane et al., 2002) after the removal of organic matter and carbonate by treating with hydrogen peroxide (15%) and acetic acid (25%), respectively. The extracted clay minerals were smeared on glass slides after being fully dispersed by an ultrasonic cleaner. Samples were then dried at room temperature. Clay mineral analysis was conducted by X-ray diffraction (XRD) using a D8 ADVANCE diffractometer with CuKα (alpha) radiation (40 kV, 40 mA) in the laboratory of the Institute of Oceanology, Chinese Academy of Sciences (IOCAS). Identification of clay minerals was made according to the position of the (001) series of basal reflections on the three XRD diagrams (Moore and Reynolds, 1989). Semi-quantitative estimates of peak areas of the basal reflection for the main clay mineral groups (smectite-17 Å, illite-10 Å, and kaolinite/chlorite-7 Å) were carried out on the glycolated samples using Topas 2P software with the empirical factors of (Biscaye, 1965). Replicate analysis of the same sample produced results with a relative error margin of ± 5%.

3. Results

Downcore variations of major and trace elemental concentrations as well as grain size of terrigenous materials at IODP Site U1429 are shown in Fig. 2 and Table S1. Based on the clear changes in grain size and geochemistry, the section can be divided into two units (Unit 1, ~34–8 ka; Unit 2, ~8–0 ka) (Fig. 2). In general, the terrigenous mean grain size of Unit 2 is coarser than Unit 1. The mean grain size of Unit 1 shows a relatively stable trend, with an average value of 10.9 μm, despite some fluctuations in the late last glacial (~34–29 ka) and middle deglacial to early Holocene (~15–8 ka). In contrast, the mean grain size rapidly increased at ~9–8 ka (Unit 1), and then gradually decreased (Fig. 2). Downcore variations in elemental concentrations are also shown in Fig. 2. The changes of major elements including CaO and Na_2O, as well as rare earth element (REE) Yb, show a similar trend as the mean grain size, with higher concentrations in Unit 2 than in Unit 1. Al_2O_3, K_2O and La have similar trends, which exhibit slightly lower concentrations in Unit 2 than those in Unit 1. Furthermore, two obvious fluctuations at ~33–29 and ~15–8 ka are recognized. The Sm and Gd show parallel trends, with slightly lower concentrations in Unit 1 than in Unit 2 (Fig. 2). Significant fluctuations in a range of ~1 ppm were found during ~15–8 ka. The upper continental crust (UCC) (Taylor and McLennan, 1985) -normalized REE compositions of the IODP Site U1429 sediments are shown in Fig. 3. Different REE patterns are recognized in Units 1 (Fig. 3A) and 2 (Fig. 3B). It is noteworthy that most samples from Unit 1 are characterized by relatively flat REE patterns with a slightly negative Ce anomaly and a strongly positive Gd anomaly. In contrast, Unit 2 differed significantly, with many samples showing relative enrichment in heavy REEs. Such samples also have coarser mean grain size (Table S1). The REE compositions of surface sediments in the Yellow River drainage basin are shown in Table S1, which characterized by relative enrichment in light REEs with slightly positive Sm anomaly, except for samples from Lanzhou, Jundu and Tongguan have the positive Eu anomaly (Table S1).

The clay mineral distribution pattern in the Yellow River drainage basin shows an increasing trend in smectite from the upper to lower reaches. The lowest content of smectite was found at Guide (10%), and the highest in Pingyin (38%) (Table 1). In contrast, illite exhibits the opposite trend, with gradually decreasing contents from the upper to lower reaches. The highest and lowest contents of illite have been found in Guide (73%) and Pingyin (47%), respectively. Chlorite shows a slightly decreasing trend from upper to lower reaches, with the highest content at Guide (12%) and Lanzhou (12%) and the lowest contents at Jundu (8%) and Pingyin (8%). Overall, kaolinite exhibits a slightly increasing trend from the upper to lower reaches, except for at Lanzhou where contents are notably high (8%) (Table 1).

4. Discussion

4.1. Sediment provenance discrimination

Interpretation of the geochemical trends as weathering records is made possible by constraining where the sediments are sourced. The REEs have been widely applied as provenance tracers in East Asian marginal seas (Dou et al., 2010a; Huang et al., 2016; Um et al., 2015). Many factors, including parent rocks, hydrological sorting and chemical weathering process are all responsible for REE composition of the marginal seas clastic sediments (Clift, 2016; Dou et al., 2010a). However, provenance is often considered to be the single most important factor influencing the sediment REE composition (Song and Choi, 2009; Taylor and McLennan, 1985; Yang et al., 2002).

In this study, the bulk sediment samples were leached with HCl before measuring the REE concentrations. This chemical pretreatment

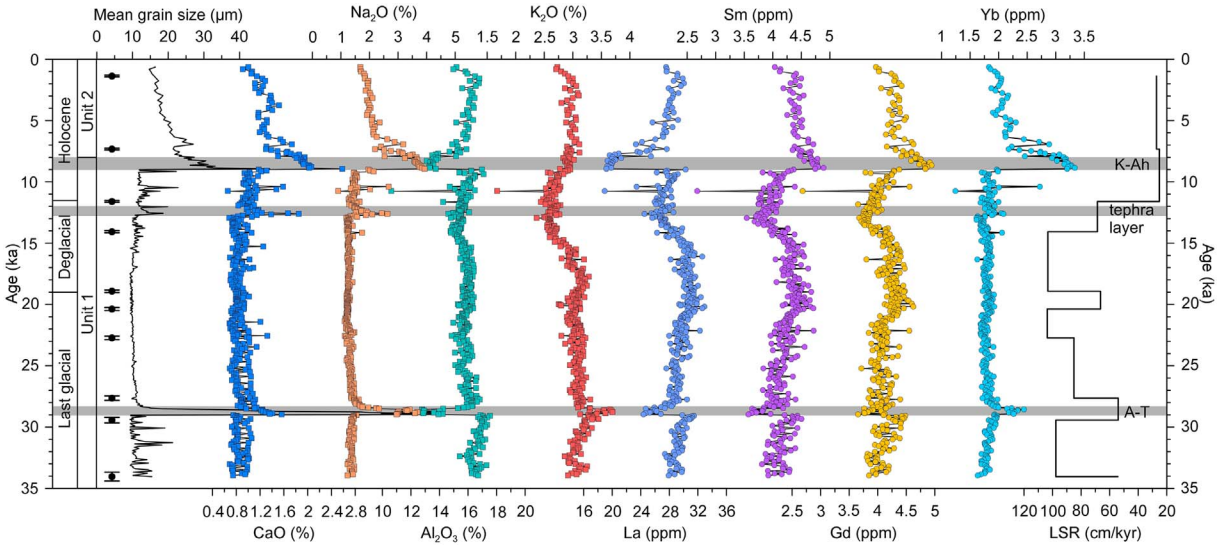

Fig. 2. Downcore variations of major and trace elemental concentrations in the sediments of IODP Site U1429 with mean grain size and linear sedimentation rates during the last 34 ka. The gray bar indicates tephra layers. Black dots show 10 Accelerator Mass Spectrometry (AMS) ^{14}C dates with an uncertainty of 2σ.

effectively removes most of the biogenic/authigenic materials in the sediments, including carbonate, organic matters, apatite, and Fe-Mn oxides, excepting for bigenic opal, based on observations by microscope. Therefore, the measured REE compositions overall represent only the contributions of the siliciclastic fraction to the core sediments. Chemical weathering thus exerts a weak influence on the REE compositions in the residual fractions (Dou et al., 2010a).

We can test the possible influence of hydrological sorting on the sediment REE composition by correlation analysis of LREEs, HREEs, $(La/Sm)_{UCC}$ and $(Gd/Yb)_{UCC}$ with terrigenous mean grain size (Fig. 4). For Unit 1, no clear correlations were observed between LREEs, HREEs, $(La/Sm)_{UCC}$, (Gd/Yb) and mean grain size (Figs. 4A and B), suggesting that grain size is not important in controlling the REE compositions of Unit 1 sediments. In contrast, the values of LREEs, $(La/Sm)_{UCC}$ and $(Gd/Yb)_{UCC}$ in Unit 2 show significant negative correlations with mean grain size, whereas the HREEs show positive correlation (Figs. 4C and D). However, we note that sediments layers with coarser grain size exhibit similar UCC-normalized REE patterns with volcanic rocks of the Kyushu Island, which are characterized by HREEs enrichment (Table S1, Fig. 3B). Therefore we suggest that the volcanic contributions are responsible for the coarser grain size and REE variability in Unit 2, and then provenance rather than hydrological sorting would dominate the REE composition of Unit 2.

The potential provenances of siliciclastic sediments in the Okinawa Trough include suspended sediments from the Yellow and Yangtze Rivers, discharging from East Asia and short mountainous rivers (i.e, Japanese or even Taiwanese rivers) from the surrounding islands, as well as eolian dust, volcanic and hydrothermal materials. It has long been suggested that the terrigenous sediments in the Okinawa Trough are mainly derived from the Yangtze and Yellow Rivers, and Taiwan-derived sediments were also transported northward from the southern Okinawa Trough by the Kuroshio Current after about 7 ka, or throughout the last glacial period (Diekmann et al., 2008; Dou et al., 2010b; Xu et al., 2014; Zheng et al., 2016). For the East Asian large rivers with the wide drainage basins, the composition of sediment transported to the sea can be changed by the relative sediment input from different catchments. It has been suggested that East Asian monsoon variability can strongly influence the mixing proportions of Yellow River sediments from the different tributaries on glacial-interglacial timescales, which resulted in the varied composition of sediment

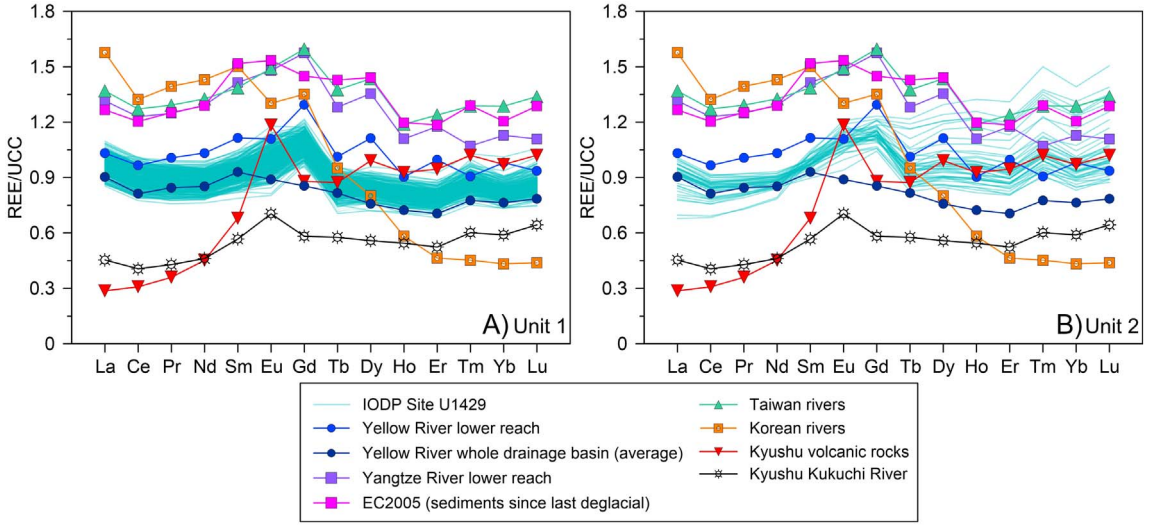
REE/UCC
A) Unit 1
B) Unit 2
La Ce Pr Nd Sm Eu Gd Tb Dy Ho Er Tm Yb Lu
IODP Site U1429
Yellow River lower reach
Yellow River whole drainage basin (average)
Yangtze River lower reach
EC2005 (sediments since last deglacial)
Taiwan rivers
Korean rivers
Kyushu volcanic rocks
Kyushu Kukuchi River

Fig. 3. UCC-normalized fractionation patterns of rare earth elements (REEs) in Unit 1 (A) and Unit 2 (B) of IODP Site U1429 sediments. The REE patterns of potential source areas are also compared with the core samples.

Table 1
Clay minerals contents of Yellow River drainage basin surface sediments.

Sample sites	Smectite (%)	Kaolinite (%)	Illite (%)	Chlorite (%)	Kaolinite/Illite
Guide	10	5	73	12	0.07
Lanzhou	15	8	65	12	0.12
Qingtongxia	18	5	65	11	0.08
Zhaojunmu	17	5	69	9	0.07
Jundu	31	6	56	8	0.10
Tongguan	27	7	55	10	0.14
Huayuankou	31	5	56	9	0.09
Pingyin	38	7	47	8	0.14
Beizhen	31	6	54	9	0.11
Lijin	33	5	52	10	0.09
Kenli	30	7	54	9	0.14

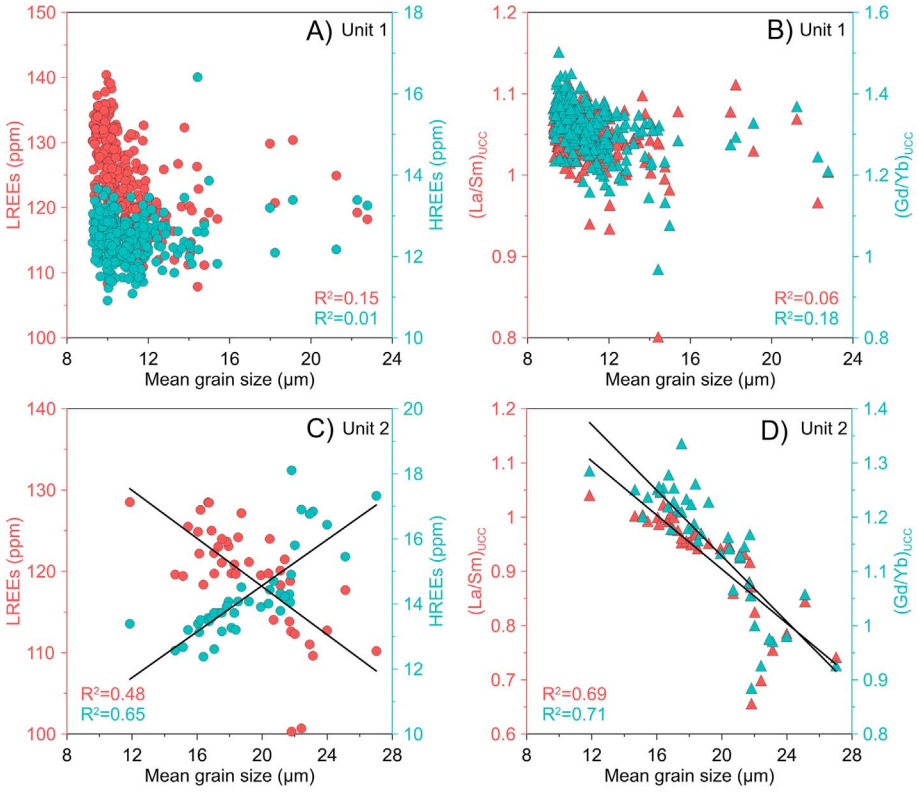

Fig. 4. Correlation plots of mean grain size with REE parameters including LREEs, HREEs, $(La/Sm)_{UCC}$ and $(Gd/Yb)_{UCC}$ for the sediments in IODP Site U1429 in Unit 1 (n = 329) (A and B) and Unit 2 (n = 42) (C and D). P-values of mean grain size vs. LREEs, $(La/Sm)_{UCC}$ and $(Gd/Yb)_{UCC}$ plots are all 0.00, and P-value of mean grain size vs. HREEs plot is 0.13 in Unit 1. P-values of mean grain size vs. LREEs, HREEs, $(La/Sm)_{UCC}$ and $(Gd/Yb)_{UCC}$ plots are all 0.00 in Unit 2.

transported to the sea during the late Quaternary (Hu, B., et al., 2012). Recently, Bi et al. (2017) showed that the provenance of sediments accumulated in the Yangtze Estuary gradually changed from the upper catchment to the mid-lower valley and shifted back to the upper catchment again during the Holocene. Therefore caution should be exercised in the use of modern river sediments as the end-member for potential provenance of offshore cores, especially when the river drainage basin is known to be sensitive to environment change over the studied time scale.

Recent study of Sr-Nd-Pb isotopes from IODP Site U1429 suggests that the contribution of suspended sediments from the rivers of Kyushu to the study area cannot be neglected (Zhao et al., 2017). In contrast, the influence of eolian dust from Central Asia to the East Asian marginal seas is insignificant because of the dominance of fluvial input (Dou et al., 2010a; Li et al., 2015; Wan et al., 2007), although it indeed plays an important role in detrital fluxes to the pelagic Pacific Ocean (Jones et al., 2000; Nakai et al., 1993). In any case, hydrothermal input is not considered to be a notable influence on sediment composition because there is no hydrothermal activity close to the study area (Glasby and Notsu, 2003). Volcanic ash is another potential sediment source to the northern Okinawa Trough, but only becomes important in sediments around the tephra layers (Chang et al., 2015; Xu et al., 2014). Invisible dispersed tephra is present but rare in the sediment (Tada et al., 2014).

Here we compare UCC-normalized REE patterns of IODP Site U1429 samples with potential sources, including sediments from the Yellow River lower reach (Yang et al., 2002), Yellow River whole drainage basin, Yangtze River lower reach (Yang et al., 2002), core EC2005 sediments since the last deglacial (Xu et al., 2011), Taiwanese rivers (Li et al., 2013), Korean rivers (Lee et al., 2008), Kyushu Kukuchi River and Kyushu volcanic rocks (Shinjo et al., 2000) (Fig. 3 and Table 2). It is obvious that samples in Unit 1 have similar patterns to the Yellow River sediments, whereas many samples in Unit 2 exhibit similar patterns to Kyushu volcanic rocks and Kukuchi River (Fig. 3), exhibiting relative enrichment in heavy REEs. Such features indicate distinct sources for the two units at Site U1429. Besides, the total REE concentration of Unit 2 are higher than Kyushu volcanic rocks and Kukuchi River, which probably suggests the mixed sources of East Asian rivers and Kyushu Island end-members.

The discrimination plot of $(La/Sm)_{UCC}$ vs. $(Gd/Yb)_{UCC}$ for IODP Site U1429 samples was further used to compare with potential sources in order to constrain the sediment provenance at the study site (Fig. 5). Here we adopted the Yellow River whole drainage basin surface

Table 2
Comparison of rare earth element compositions between IODP Site U1429 sediments with potential end-members.

Samples	Depth (m)	Age (ka)	ΣREE (ppm)	HREEs (ppm)	LREEs (ppm)	$(La/Yb)_{UCC}$	$(Gd/Yb)_{UCC}$	$(La/Sm)_{UCC}$
Unit 1	0–2.17	0–7.95	129.3	14.3	115.1	0.93	1.15	0.93
Unit 2	2.22–18.89	8.05–33.95	132.8	12.4	120.4	1.19	1.32	1.05
Whole core	0–18.89	0–33.95	132.4	12.6	119.7	1.16	1.30	1.03
UCC	–	–	146.4	13.9	136.3	1.00	1.00	1.00
Yellow River	Surface sediment	Modern	138.7	14.5	124.1	1.03	1.32	0.92
Yellow River upper reach	Surface sediment	Modern	125.7	10.6	115.1	1.23	1.09	1.00
Yellow River middle reach	Surface sediment	Modern	113.6	10.2	103.4	1.20	1.20	0.93
Yellow River lower reach	Surface sediment	Modern	127.5	11.5	116.0	1.12	1.09	0.97
Yangtze River	Surface sediment	Modern	188.9	18.6	170.4	1.17	1.40	0.93
Taiwan rivers	Surface sediment	Modern	193.0	21.0	172.0	0.93	1.04	0.95
Korean rivers	Surface sediment	Modern	243.6	12.4	231.2	4.93	3.91	1.11
Kukuchi River	Surface sediment	Modern	65.7	7.9	57.8	0.77	0.99	0.80
Kyushu volcanic rocks	–	–	59.9	9.8	50.1	0.29	0.90	0.42

Note: ΣREE denotes total REE concentrations (ppm); $(La/Yb)_{UCC}$, $(Gd/Yb)_{UCC}$ and $(La/Sm)_{UCC}$ refer to the UCC-normalized REE fractionation parameters. Volcanic rocks from the Okinawa Trough. Data sources: Yellow River, Yangtze River (Yang et al., 2002), Taiwan rivers (Li et al., 2013), Korean rivers (Lee et al., 2008), Kyushu volcanic rocks (Shinjo et al., 2000), UCC (Taylor and McLennan, 1985).

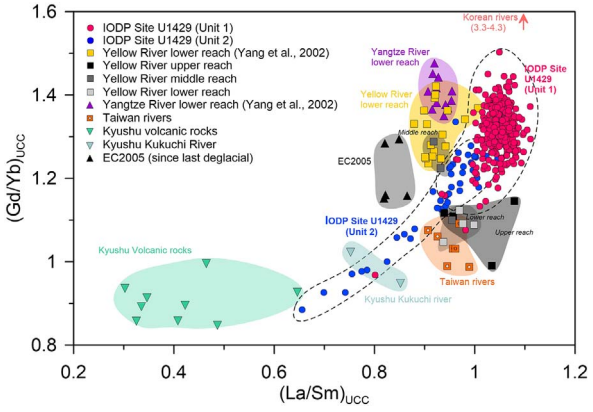

Fig. 5. Discrimination plot of $(Gd/Yb)_{UCC}$ vs. $(La/Sm)_{UCC}$ for the sediments of IODP Site U1429. Values of modern sediments from Yellow River and Yangtze River lower reaches (Yang et al., 2002), Yellow River whole drainage basin, EC2005 sediments since the last deglacial (Xu et al., 2011), Taiwan rivers (Li et al., 2013) and Korean rivers (Lee et al., 2008), Kyushu Kukuchi River, as well as Kyushu volcanic rocks (Shinjo et al., 2000) are also compared with the core samples.

sediment samples to trace whether the sediment mixing proportions of different catchments over the study time scale could influence the sediment evolution of the study core. The sediment core EC2005 located in the south of Yangtze River estuary was chosen as the analogue of Yangtze River end-member on the geological time. The sediments of the core were mainly transported from the Yangtze River catchment by the coastal current since the last deglacial (Xu et al., 2011). The Kyushu Island end-member was represented by the Kyushu volcanic rocks and Kukuchi River sediment. However, as shown in the $(La/Sm)_{UCC}$ vs. $(Gd/Yb)_{UCC}$ plot (Fig. 5), the REE compositions of surface sediment in the Yellow River lower reach in previous study (Yang et al., 2002) are different from the lower reach sediment in this study, but similar to the Yellow River middle reach sediment in this study. Such difference probably resulted from the different sampling seasons/years. It has been suggested that the Yellow River runoff changed significantly during the past decades (Wang et al., 2013). Samples in this study were collected in 1983, when the Yellow River suggested a relative higher runoff ($\sim 450 \times 10^8$ m^3/a in the upper reach and $\sim 540 \times 10^8$ m^3/a in the middle reach), comparing with the sampling time of Yang et al. (2002), which collected in 1997–2000 with the lower river runoff ($\sim 330 \times 10^8$ m^3/a in the upper reach and $\sim 150 \times 10^8$ m^3/a in the middle reach) (Kang et al., 2005; Wang et al., 2013). Our samples collected in a high runoff year probably induced relative more sediment transported from upper to the lower reach, and thus resulted in the similar REE composition between these two regions. This should be the main reason for the difference of REE composition in lower reach sediments between this and previous studies (Fig. 5). Besides, sediments in the lower reach should mainly come from middle reach in a lower runoff year due to the dominantly sediment load of the middle reach (Ren and Shi, 1986), which induced the similar REE composition of sediments between middle reach in this study and lower reach in previous study (Yang et al., 2002) (Fig. 5). For the study site, Unit 1 samples mainly fall in a cluster close to the Yellow River middle reach or Yellow River lower reach (Yang et al., 2002), which suggests that Yellow River middle reach sediments dominated the terrigenous supply during this period.

For the Unit 2, all the samples plot as a band between the Yellow River and Kyushu volcanic rocks, which display a trend extending from the Yellow River middle to the upper reaches, and toward the volcanic rocks, which indicate significant influence of Kyushu-derived materials, and the increased contribution from the Yellow River upper reach (Fig. 5). In general, the samples clearly deviate from the Yangtze River, Taiwanese and Korean river sediments in both Units 1 and 2. Therefore, we conclude that the sediments in Unit 1 (~34–8 ka) at IODP Site U1429 mainly come from the Yellow River middle reach, whereas Unit 2 (~8–0 ka) experienced stronger influence from the upper reach of the Yellow River and Kyushu-derived sediments.

4.2. Sediment transport processes and controlling mechanisms

The transport of terrigenous sediments in the East China Sea is dominantly influenced by changes in sea level, ocean currents and monsoon climate (Diekmann et al., 2008; Dou et al., 2016; Zheng et al., 2016). During the last glacial and deglacial period (~34–8 ka, Unit 1), prominent sea-level fall led to the progradation of the coastline and exposure of the East China Sea shelf. In recent years, paleo-Yellow River channels have been found in the south Yellow Sea shelf and northern East China Sea shelf (Liu et al., 2010) (Fig. 1A). As a result, the paleo-Yellow River mouth must have been positioned significantly closer to the northern Okinawa Trough at that time. This situation favors large fluvial discharge or even direct input of detrital sediments from the paleo-Yellow River to the study area. Previous studies suggested that enhanced East Asian summer monsoon precipitation would be expected to increase physical erosion rate in East Asia on millennial scales (Colin et al., 2010; Hu et al., 2013; Wan et al., 2015). If that is true then weakened precipitation in Kyushu (~5 mm/day lower than today in summer season (Ju et al., 2007)) should have resulted in relative low input of Kyushu sediments to the study site during the last glacial and deglacial periods. For the Yellow River, simulated annual precipitation in the southern Yellow Sea and northern East China Sea shelves during the Last Glacial Maximum was about 450–650 mm, which is higher

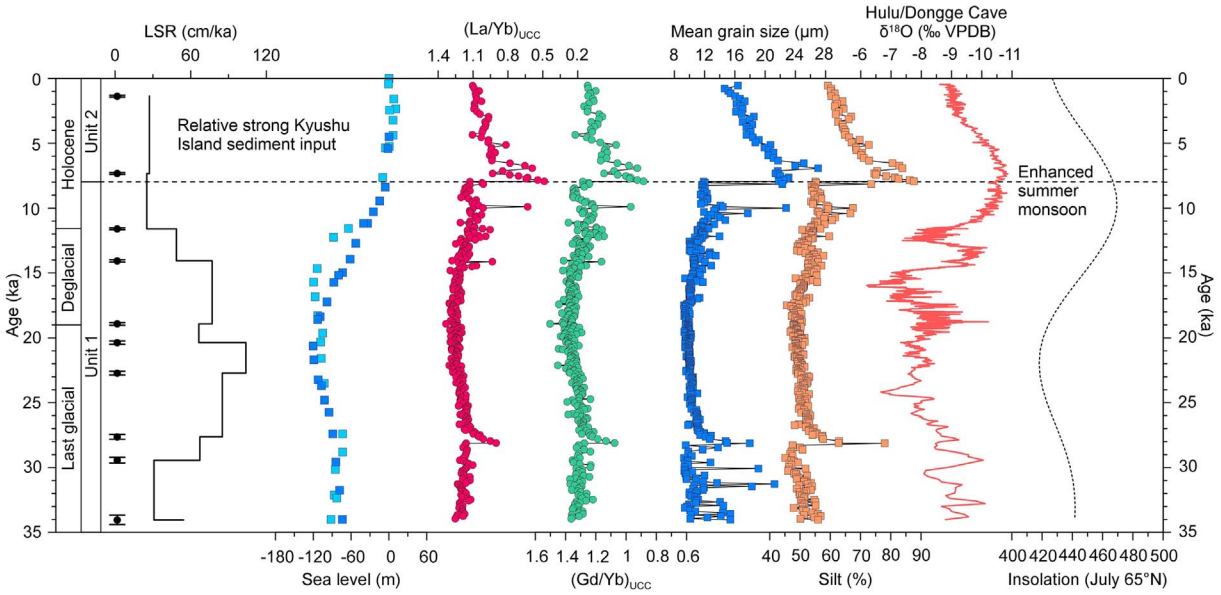

Fig. 6. Comparison of IODP Site U1429 sediment parameters, including LSR, $(La/Yb)_{UCC}$, $(Gd/Yb)_{UCC}$, mean grain size and silt content, with the sea-level change (Cutler et al., 2003; Saito et al., 1998), $\delta^{18}O$ records of Hulu and Dongge caves (Dykoski et al., 2005; Wang et al., 2001) and the summer isolation at 65°N (Berger and Loutre, 1991) since the last 34 ka. The dash line shows the boundary between Unit 1 and Unit 2. Black dots show 10 Accelerator Mass Spectrometry (AMS) ^{14}C dates with an uncertainty of 2σ.

than the annual precipitation (200–600 mm) in the present Yellow River drainage (Ju et al., 2007). Therefore, there were still considerable rainfall to deliver sediments from Yellow and East China Sea shelves to the northern Okinawa Trough through the paleo-Yellow River channels during the late last glacial. Lower sea level, together with monsoon precipitation patterns, induced a dominant Yellow River sediment input at ~34–8 ka (Fig. 6).

It has been suggested that the Yellow River mouth gradually retreated with rising sea level and reached its present position at about 8.5 ka (Saito et al., 2000). The pattern of modern oceanic circulation in the East China Sea was established at about 7.5–6.0 ka (Ujiie et al., 1991). Yellow River sediments have mostly been deposited near the modern river mouth and around the Shandong Peninsula, with fine-grained particles transported southward along the coast by the Yellow Sea Coastal Current (Milliman et al., 1989). Accordingly, because of the longer distance from the Yellow River mouth to the study area that accompanied rising sea level and accounting for the "blocking effect" of the Kuroshio Current branches (Dou et al., 2010b; Guo et al., 2001; Zheng et al., 2016), the flux of Yellow River-derived materials into the northern Okinawa Trough largely decreased after ~8 ka (Fig. 6). In contrast, sediment input from Kyushu to the northern Okinawa Trough was only slightly influenced by the sea-level change because of the narrow continental shelf associated with that island (< 50 km). It has been suggested that strong rainfall results in frequent landslides and debris flow on Kyushu (Kasai et al., 2004; Sidle and Masahiro, 2004), which favor production and transport of coarse-grained sediments to the northern Okinawa Trough. Although a strengthened Kuroshio Current and its branches can block the transport of Kyushu sediments to the western side of the Okinawa Trough (Li and Chang, 2009), such a blocking effect probably mainly acted on the fine-grained input from Kyushu (Li and Chang, 2009; Zhao et al., 2017). As a result, the strengthened East Asian summer monsoon induced stronger weathering and erosion during the Holocene compared to the last glacial and this can account for the increased input of Kyushu sediment to the study site. Accordingly, the coarser mean grain size and higher silt content, as well as the lower $(La/Yb)_{UCC}$ and $(Gd/Yb)_{UCC}$ indicate relatively strong sediment supply from Kyushu compared to the Yellow River since ~8 ka (Fig. 6).

Comparing with the last glacial and deglacial, the large scale glacier melt in the eastern Tibet near the Yellow River source during the Holocene supplied more water discharge (Zhang and Mischke, 2009), and thus transported more upper reach river materials to the downstream. However, the accumulation rate of loess materials in the middle reach of Yellow River was lower than that in the glacial and deglacial (Sun et al., 2006). Such varied condition could induce increased contribution of upper reach materials comparing to the middle reach in the total sediment budget of Yellow River. Even the enhanced East Asian summer monsoon rainfall could intensify the erosion on the Loess Plateau, however, this increase probably was less than the glacier melt water induced-sediment erosion in the upper reach according to our provenance result.

4.3. Weathering proxies

Weathering products comprise the majority of the detrital components in the sediments considered here. Chemical signatures induced by paleoenvironmental change in the source regions are ultimately transferred to the sedimentary records (Nesbitt and Young, 1982). Consequently, we select a series of elemental ratios and proxies to constrain variations in the intensity of chemical weathering, and thus reconstruct the paleoenvironmental evolution. Behaviors of elements are distinct during the chemical weathering process. In general, alkalis and alkaline earth elements are easily removed with primary minerals during chemical weathering. In contrast, other elements, such as Al, Fe and Ti tend to be combined in secondary minerals and thus to be retained in the soil profile (Nesbitt and Markovics, 1997). The chemical weathering intensity of the sediments can be deduced by a quantitative estimation of the chemical weathering of silicates, such as the calculated values of chemical index of alteration (CIA) (Nesbitt and Young, 1982). CIA is defined as $Al_2O_3/(Al_2O_3 + CaO^* + Na_2O + K_2O) \times 100$ (molar content; CaO* is the CaO content in the silicate fraction of the sample), which has long been used as a quantitative estimation of the chemical weathering intensity, based on the relative mobility of Na, K and Ca in aqueous fluids compared to immobile Al (Clift et al., 2014; Dou et al., 2016; Nesbitt and Young, 1982; Wan et al., 2010). In addition, chemical weathering intensity can also be calculated for individual elements (e.g., K and Mg) mobilized during incongruent weathering of silicates by comparing their concentration to that of a non-mobile element (e.g., Al) (Gaillardet et al., 1999; Garzanti et al., 2014). As a result, lower values of ratios like K/Al and Mg/Al indicate more depletion of mobile

elements in sediments and thus higher chemical alteration. Mineralogical proxies can also be adopted to reconstruct chemical weathering intensity, especially clay mineral ratios. It has been suggested that kaolinite is typically formed in soils developed in regions with warm humid climates and good drainage conditions, whereas illite is the product of physical erosion from bedrock or formed by weathering of feldspar and micas under moderate hydrolysis conditions (Chamley, 1989). Enhanced chemical weathering intensity in a given basin induces further degradation of illite to kaolinite leading to a higher kaolinite/illite ratio (Wan et al., 2015).

In addition to chemical weathering, other factors including provenance change, hydraulic sorting, as well as diagenesis and/or metasomatism after burial may also influence the elemental ratios in detrital sediments (Fralick and Kronberg, 1997). As discussed above, the composition of Unit 2 sediments has been strongly influenced by influx of Kyushu-derived materials, whereas the Unit 1 represents a relatively stable provenance with the sediments being mainly derived from the Yellow River middle reach. In order to isolate the influence of provenance change on the elemental ratios, here we exclude Unit 2 and only focus on Unit 1 in order to discuss silicate weathering and erosion during the late last glacial and deglacial. Correlation plots of CIA, K/Al, Mg/Al and kaolinite/illite vs. $(Gd/Yb)_{UCC}$ for the Unit 1 of IODP Site U1429 have been adopted to constrain the effects of provenance on element composition (Figs. 7A and B). Poor correlations have been found between $(Gd/Yb)_{UCC}$ and CIA, K/Al, kaolinite/illite, respectively, which suggests that provenance had an insignificant influence on these weathering proxies at IODP Site U1429 during the late last glacial and deglacial. However, the moderate correlation between $(Gd/Yb)_{UCC}$ and Mg/Al implies that provenance change plays a role in regulating the Mg/Al proxy (Fig. 7B). The sediment chemistry is dominated by the constituent mineral phases, and each has a characteristic grain-size range, shape and density (Wan et al., 2007). Hydraulic sorting readily selects and separates particles with similar attributes from associated but dissimilar particles. As a result, mineral particles with similar grain size, density and shape experience similar hydraulic sorting (Wan et al., 2017). Correlation plots of CIA, K/Al, Mg/Al and kaolinite/illite vs. mean grain size for Unit 1 have been used to constrain the effects of hydraulic sorting on chemical composition (Fig. 7C and D). Weak

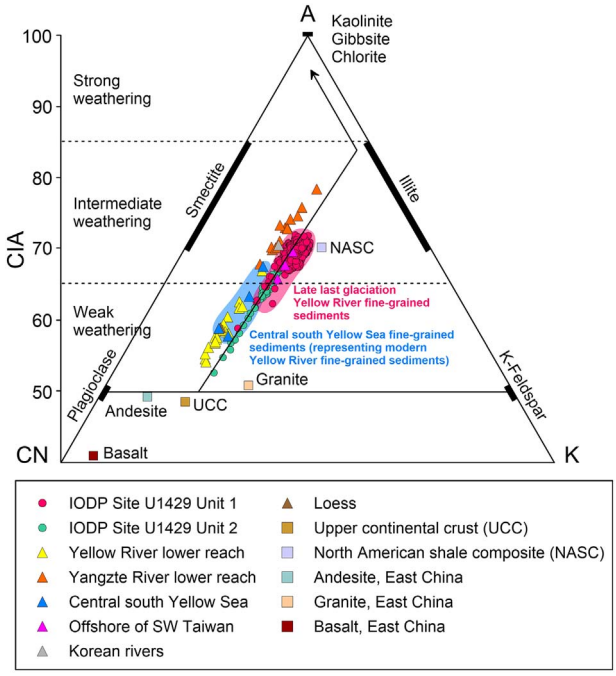

Fig. 8. Al_2O_3-(CaO^* + Na_2O)-K_2O (A-CN-K) ternary diagram of siliciclastic sediments from IODP Site U1429 Unit 1 and Unit 2. Data from the tephra and turbidity layers and overlying disturbed layers are excluded. Data of detrital sediments from Yellow River lower reaches, Yangzte River lower reaches (Yang et al., 2004a), offshore of southwestern Taiwan (Selvaraj and Chen, 2006), Korean rivers (Yang et al., 2004b), central south Yellow Sea (Yang and Youn, 2007) and Loess Plateau (Yang et al., 2004a) are plotted for comparison. Upper continental crust (UCC) (Taylor and McLennan, 1985), North American shale composite (NASC) (Gromet et al., 1984), granite, andesite, and basalt in Eastern China (Yan and Chi, 2005) are also plotted as a reference.

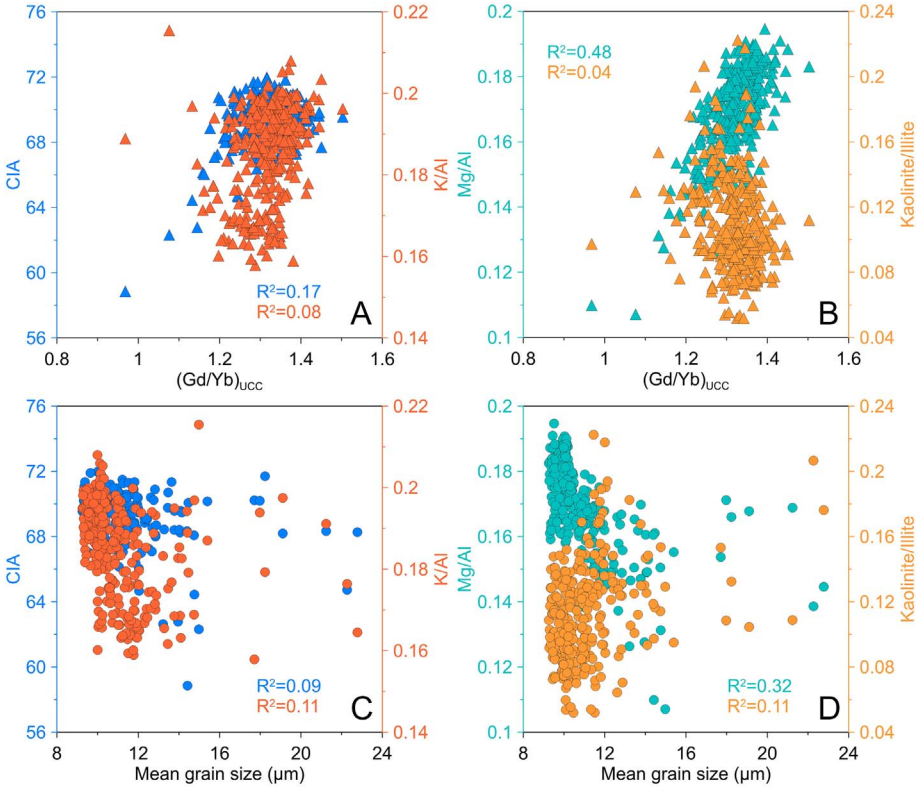

Fig. 7. Diagrams showing the relationship between the used weathering proxies (CIA, K/Al, Mg/Al and kaolinite/illite) and provenance proxy $(Gd/Yb)_{UCC}$ (A and B), mean grain size (C and D) for the sediments from IODP Site U1429 in Unit 1 (n = 329). P-values of $(Gd/Yb)_{UCC}$ and mean grain size vs. weathering proxies' plots are all 0.00.

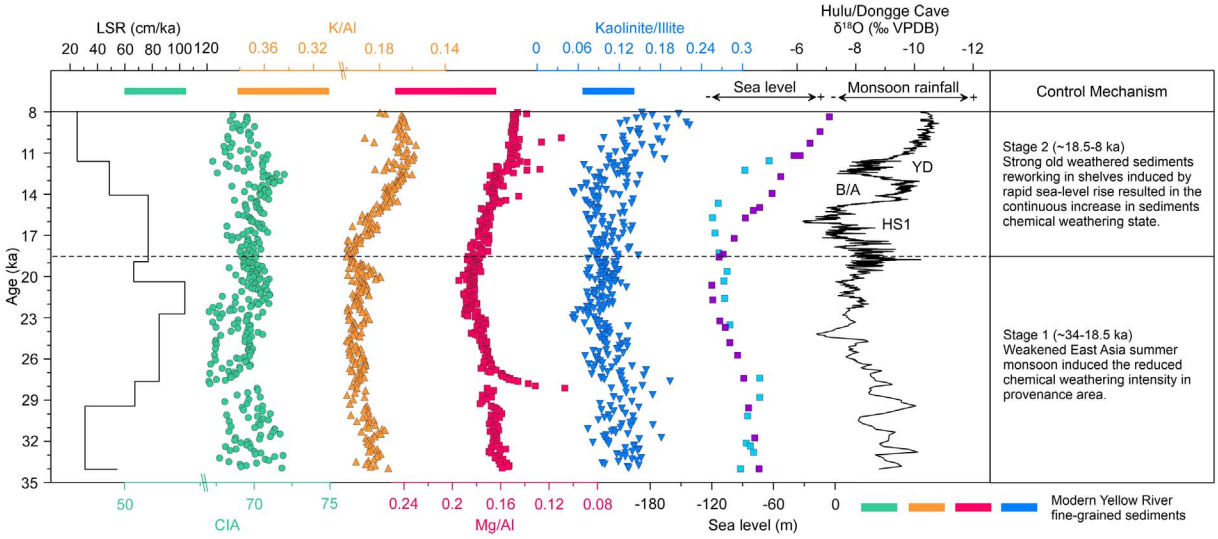
LSR (cm/ka)
20 40 60 80 100 120
K/Al
0.36 0.32 0.18 0.14
Kaolinite/Illite
0 0.06 0.12 0.18 0.24 0.3
Hulu/Dongge Cave
δ18O (‰ VPDB)
-6 -8 -10 -12
Sea level
Monsoon rainfall
Control Mechanism
YD
B/A
HS1
Age (ka)
8 11 14 17 20 23 26 29 32 35
Stage 2 (~18.5-8 ka)
Strong old weathered sediments reworking in shelves induced by rapid sea-level rise resulted in the continuous increase in sediments chemical weathering state.
Stage 1 (~34-18.5 ka)
Weakened East Asia summer monsoon induced the reduced chemical weathering intensity in provenance area.
50 70 75
CIA
0.24 0.2 0.16 0.12 0.08
Mg/Al
-180 -120 -60 0
Sea level (m)
Modern Yellow River fine-grained sediments

Fig. 9. Comparison of chemical weathering proxies (CIA, K/Al, Mg/Al and kaolinite/illite) with LSR, sea-level change (Cutler et al., 2003; Saito et al., 1998) and $\delta^{18}O$ records of Hulu and Dongge caves (Dykoski et al., 2005; Wang et al., 2001) from ~34–8 ka. Modern Yellow River fine-grained sediment weathering proxies (rectangles) have also been plotted.

correlations have been found between mean grain size and CIA, K/Al, Mg/Al and kaolinite/illite, respectively, which indicates that the hydraulic sorting had an insignificant influence on these proxies during late last glacial and deglacial times.

Previous studies suggested that alkali metal elements, such as Na and K, could be mobilized by diagenesis and/or metasomatism (Wan et al., 2010). The Al_2O_3-(CaO^* + Na_2O)-K_2O (A-CN-K) (molar content; CaO^* is the CaO content in the silicate fraction of the sample) diagram has been adopted successfully to identify metasomatic effects (Fedo et al., 1995). Unmetasomatized sedimentary rocks should plot on the predicted weathering trend that lies parallel to the A-CN axis. If there were considerable addition or substitution of Na and K, then compositions would deviate from the predicted trend and form an array oblique to the A-CN axis (Fedo et al., 1995). Samples analyzed from IODP Site U1429 plot subparallel to the A-CN axis, which indicate an absence of metasomatism, consistent with their shallow burial (Fig. 8).

We conclude that the selected geochemical proxies from Unit 1 did not vary significantly as a result of changes in provenance, hydraulic sorting, as well as diagenesis and/or metasomatism, but mainly reflect the degree of chemical alteration which may be linked to East Asian summer monsoon intensity and/or sea-level change during the late last glacial and deglacial.

4.4. Silicate weathering on glacial-interglacial timescale

Silicate weathering trends can be observed on the A-CN-K diagram (Nesbitt and Young, 1989). As shown in Fig. 8, all samples from IODP Site U1429 Unit 1 form a group plotting subparallel to the A-CN line. The trend of silicate weathering displays preferential leaching of CaO and Na_2O and enrichment of Al_2O_3, while K_2O contents almost remain constant, which suggests that plagioclase was selectively weathered first, while K-feldspar less leached. In addition, the chemical compositions of, the Yellow River lower reaches, the Loess Plateau, the Yangtze River lower reaches and offshore southwestern Taiwan fall on the similar weathering-trend as those from IODP Site U1429 (Fig. 8). The ~3–12 μm fractions of surface sediments from the central southern Yellow Sea, which represent fine-grained sediments from the modern Yellow River and exclude the possible effects of hydraulic sorting (Yang and Youn, 2007), were also plotted in the same weathering trend. Such a trend points to a gradual increase in weathering intensity for the detrital sediments from the Yellow to the Yangtze River basin. As discussed above, the sediments (mean grain size of ~11 μm) in Unit 1 (~34–8 ka) of IODP Site U1429 were mainly derived from the Yellow River middle reach, when the sediments supply was high due to the relative low sea level (Fig. 6). However, these sediments, which were deposited in a cold period, are more chemically altered than fine-grained modern Yellow River sediments, represented by the central Yellow Sea fine-grained surface sediments (i.e., deposited in warm period) (Fig. 8).

Subaerial silicate weathering is critically regulated by the temperature, precipitation, physical erosion and residence time (Kump et al., 2000; West, 2012). Generally, stronger East Asian summer monsoon precipitation and higher surface temperatures would be expected to increase chemical weathering rates in East Asia under stable tectonic conditions (Kump et al., 2000; West, 2012). Such close coupling has been demonstrated in East Asian continental drainage basins on millennial or shorter timescales, e.g., Yangtze River (Bi et al., 2015), Pearl River (Hu et al., 2013), Red River (Wan et al., 2015) and Mekong River (Colin et al., 2010). However, compared with modern Yellow River sediments, the glacial sediments from IODP Site U1429 are more chemically altered, despite sedimentation when the East Asian summer monsoon precipitation was weaker, the climate was colder (Fig. 8). To explain this weathering trend, the origin of the weathering signature observed in the detrital sediments must be evaluated.

It has been suggested that post-depositional alteration of sediments in the marine environment may affect the composition of deposited sediments (Jones et al., 2012; Scholz et al., 2013). In the subaerial environment, pedogenic processes lower the pH of pore fluids considerably, such that the rates of silicate mineral dissolution are high (Stumm and Morgan, 2012). However, in most marine pore waters, pH is relatively stable as a result of buffering (~7.2–7.6) (Aloisi et al., 2004), such that the dissolution of silicate minerals proceeds very slowly. As a result, silicate mineral weathering is a sluggish process in most marine diagenetic environments (Aloisi et al., 2004). There is no downcore trend to increasing chemical alteration (Fig. 9), suggesting that burial is not the main controlling factor over bulk sediment chemistry since the last glacial and deglacial. Submarine weathering of the sediments in the southern Okinawa Trough was not taken into account in the study conducted by (Dou et al., 2016). Here we argue that submarine silicate weathering is insignificant for the northern Okinawa Trough detrital sediments over our study time scale.

Another possibility for the weathering state is onshore weathering and erosion. Based on the sediment source tracing, the Yellow River upper and lower reaches supplied more materials to the study site during the Holocene than that in the last glacial and deglacial, which means more upper materials were transported to the central Yellow

Sea. Previous studies have estimated that ~90% of the Yellow River sediments came from the middle-upper reaches (Ren and Shi, 1986), which characterized by the fragile structure of the soils, and thus results the difficulty of the bedrock weathering in the drainage basin of the Yellow River. As a result, the mineralogical composition in the river sediments should not be determined by the bedrock but climate. According to the clay mineral contents in the Yellow River surface sediments in the whole drainage basin, increased kaolinite/illite from upper to the lower reaches indicate the enhanced chemical weathering intensity (Table 1), due to unfavorable to favorable temperature and rainfall from upper to the lower reaches. More weak weathered sediments from upper reach were transported to the sea during the Holocene than that in the last glacial and deglacial, which has been proved by the bulk chemical weathering proxies (Figs. 8 and 9). Besides, the similar chemical altering state between glacial and modern sediments indicated by kaolinite/illite probably indicates the small amount of clay-sized sediment supply from upper reach, relative higher clay-sized sediment load from middle or/and lower reaches which characterized by the higher altering state probably account for the similar chemical weathering state between the glacial and Holocene sediments. Therefore, the provenance change should be a main reason for the higher alteration state of sediments deposited in the last glacial and deglacial than that in the Holocene.

The pre-depositional subaerial processes have been proposed to be the main reason for the enhanced chemical weathering state of tropical shelf sediment during glacial lowstands (Wan et al., 2017). During times of low sea levels, terrigenous sediments were eroded from the exposed continental shelf and redeposited on the lower slope and deep basin (Hu, D., et al., 2012; Limmer et al., 2012). Thus the weathering state of shelf sediments is a composite effect of weathering during interglacial sediment production and additional weathering upon subaerial exposure of shelf deposits during glacial lowstand periods (Wan et al., 2017). It has been noted that the simulated annual precipitation and annual mean temperature in the southern Yellow Sea and northern East China Sea shelves during the Last Glacial Maximum was about 450–650 mm and 5–10 °C, respectively (Ju et al., 2007). This is higher than the annual precipitation (200–600 mm) and similar to the annual mean temperature (5–10 °C) in the present Yellow River drainage (Ju et al., 2007). The permeable sediments exposed on the mid-latitude continental shelf during times of low sea level have the right environmental conditions to be weathered further than experienced during their initial phase of erosion and transport. The shelf sediments would have experienced more precipitation and similar temperatures as the modern Yellow River drainage basin. Besides, given the flat terrain and sufficient duration, a huge reactive area in the Yellow Sea and East China Sea shelves (about 9×10^5 km^2) (Qin et al., 1989; Qin, 1996) would have been available for alteration. However, this effect would be expected to be much weaker than that in tropical shelves with warmer and more humid conditions (Wan et al., 2017). In any case, the last deglacial sea-level rise could also induce strong reworking along the continental shelf edge (Dou et al., 2010b), and resulted in an enhanced alteration of the sediments then deposited in the deep basin (Dou et al., 2016; Hu, D., et al., 2012). All the factors discussed above could account for the enhanced alteration state of the IODP Site U1429 sediments during the last glacial and deglacial compared to the modern Yellow River.

In summary, we argue that provenance change was the main reason for enhanced alteration state of the IODP Site U1429 sediments during the last glacial and deglacial compared to the modern Yellow River. In addition, the pre-depositional subaerial processes could also account for this to some extent. However, it's difficult to identify these two processes using the available data.

4.5. Silicate weathering on multi-millennial timescale

As shown in Fig. 9, the geochemical and clay mineral proxies reveal consistent variation between the last glacial and deglacial, during which time provenance was stable and sediment was primarily supplied from the Yellow River. In general, K/Al, Mg/Al and kaolinite/illite values show that the terrigenous alteration during this period can be divided into two stages: stage 1 (~34–18.5 ka), characterized by relatively weak and decreasing chemical weathering intensity; stage 2 (~18.5–8 ka), with relatively strong and increasing weathering intensity. It has been discussed above that the contribution of Kyushu sediments to the northern Okinawa Trough became stronger after the late deglacial because of strengthened East Asian summer monsoon precipitation and sea-level rise. The introduction of Kyushu-derived sediments probably caused the disunity (CIA and other proxies) of the chemical proxies from ~11 to 8 ka. The Kyushu sediment end-member has higher concentration of CaO and Na_2O, and similar concentration of K_2O, Al_2O_3 and MgO comparing with the core sediments (Table S1). The slightly increased Kyushu materials relative input since the late deglacial and early Holocene induced more sediment with higher CaO and Na_2O to the northern Okinawa Trough, and thus could result the CIA decoupled with other chemical weathering proxies since ~12 ka.

It has long been suggested that climate (i.e., mean temperature and precipitation) is the primary driving mechanism for chemical weathering in monsoon-dominated river basins (Bi et al., 2015; Dou et al., 2016; Wan et al., 2015). From ~34 to 18.5 ka, CIA, K/Al, Mg/Al and kaolinite/illite correlate with the rainfall signal inferred from the Hulu and Dongge Cave speleothem isotopic records (Dykoski et al., 2005; Wang et al., 2001). A cooling and drying climate is associated with weakened summer monsoon activity and is consistent with the reduced alteration of sediments eroded from Yellow River basin. This implies that summer monsoon precipitation was the primary controlling factor on the chemical weathering intensity of sediments deposited during this period. The increasing sedimentation rate from ~34 to 18.5 ka does not indicate faster sediment transfer or shorter residence time in the terrestrial catchment resulting in reduced sediment alteration due to the weakened precipitation. The fall of sea level caused the paleo-Yellow River mouth to approach the Okinawa Trough gradually, which would account for the increased sedimentation rate at the core site during this period.

From ~18.5 to 8 ka around the last glacial termination, the East Asian summer monsoon experienced significant fluctuations during Heinrich event 1, the Younger Dryas and Bølling-Ållerød warming (Andersen et al., 2004; Wang et al., 2001). However, chemical alteration continuously increased, consistent with coherent variation driven by sea-level rise (Fig. 9). It has been argued that rapid sea-level rise during the transitions from the glacial to Holocene could induce strong reworking of the old weathered sediments in the East Asian marginal sea shelf edge (e.g.,Tjallingii et al., 2010; Dou et al., 2010b), driving transport of these sediments to the deep basin and resulting in enhanced silicate alteration of the sediments (Dou et al., 2016; Hu, D., et al., 2012). Thus, we propose that the sea-level change during the glacial termination, overwhelming the East Asian summer monsoon variability, has become the primary control on the sediment alteration state at the study site.

5. Conclusions

High-resolution geochemical proxies for silicate weathering derived from the major and trace element composition, as well as from high resolution grain-size data were measured in terrigenous sediments from the Integrated Ocean Drilling Program (IODP) Site U1429 in the northern Okinawa Trough since 34 ka.

Provenance proxies indicate that these sediments were mainly transported from the Yellow River and Kyushu. During ~34–8 ka, relatively low sea level and proximity of the paleo-Yellow River mouth to the northern Okinawa Trough induced a dominant Yellow River middle reach sediment input. After ~8 ka, the Yellow River mouth retreated and the Kuroshio Current acting in a blocking fashion, resulting in a

significant reduction of sediment input from the Yellow River. Together with strong East Asian summer monsoon precipitation resulted in relatively strong sediment input from Kyushu to the northern Okinawa Trough. Besides, the large scale glacier melt in the Yellow River source areas and enhanced East Asian summer monsoon rainfall induced more upper reach materials to be transported to the study site.

On glacial-interglacial scale, IODP Site U1429 sediments deposited at ~34–8 ka were more strongly chemically altered compared to modern Yellow River sediments. We attribute this difference to a stronger erosion of weak weathered sediments from upper reach to the sea during the Holocene than that in the last glacial and deglacial. Besides, composite effect of weathering during interglacial sediment production and additional weathering upon subaerial exposure of shelf deposits, as well as the more favorable conditions (higher precipitation amounts and similar temperature compared with the modern Yellow River drainage basin) on the exposed southern Yellow Sea and northern East China Sea shelves during the low sea-level stage, and reworking of old weathered sediments during sea-level rise may also have played a part in causing this trend during the last deglacial and early Holocene. On multi-millennial scale, silicate weathering of IODP Site U1429 sediments was mainly controlled by the East Asian summer monsoon during ~34–18.5 ka. From ~18.5 to 8 ka, rapid sea-level rise resulted in reworking of old weathered sediments and relatively reduced input of fresh terrestrial sediments to the northern Okinawa Trough. Together these processes overwhelmed the effect of the East Asian summer monsoon on the silicate weathering process. This resulted in a continuous increase in chemical weathering state in the sediments during this period.

Supplementary data to this article can be found online at https://doi.org/10.1016/j.palaeo.2017.11.002.

Acknowledgments

We acknowledge the Integrated Ocean Drilling Program and the scientific party and technicians of IODP Expedition 346 for recovering the samples. We thank Dr. Yoshimi Kubota in National Museum of Nature and Science, Japan, for helping collecting the sediment samples of Kyushu Kukuchi river. We thank the editors Thomas Algeo and Thierry Correge, and two anonymous reviewers for their constructive comments. This work was supported by the National Natural Science Foundation of China (41622603, 41576034, U1606401), National Program on Global Change and Air-Sea Interaction (GASI-GEOGE-03), Innovation Project (2016ASKJ13) and Aoshan Talents program (2017ASTCP-ES01) of Qingdao National Laboratory for Marine Science and Technology and CAS Interdisciplinary Innovation Team. PC wishes to thank the Charles T. McCord Jr. chair in petroleum geology for his involvement in this project.

References

Aloisi, G., Wallmann, K., Drews, M., Bohrmann, G., 2004. Evidence for the submarine weathering of silicate minerals in Black Sea sediments: possible implications for the marine Li and B cycles. Geochem. Geophys. Geosyst. 5 (4).
Andersen, K.K., Azuma, N., Barnola, J.M., North Greenland Ice Core Project Members, 2004. High-resolution record of Northern Hemisphere climate extending into the last interglacial period. Nature 431 (7005), 147–151.
Berger, A., Loutre, M.-F., 1991. Insolation values for the climate of the last 10 million - years. Quat. Sci. Rev. 10 (4), 297–317.
Berner, R.A., Berner, E.K., 1997. Silicate Weathering and Climate, Tectonic Uplift and Climate Change. Springer, pp. 353–365.
Bi, L., Yang, S., Li, C., Guo, Y., Wang, Q., Liu, J.T., Yin, P., 2015. Geochemistry of river-borne clays entering the East China Sea indicates two contrasting types of weathering and sediment transport processes. Geochem. Geophys. Geosyst. 16 (9), 3034–3052.
Bi, L., Yang, S., Zhao, Y., Wang, Z., Dou, Y., Li, C., Zheng, H., 2017. Provenance study of the holocene sediments in the changjiang (yangtze river) estuary and inner shelf of the east china sea. Quat. Int. 441, 147–161 (Part A).
Biscaye, P.E., 1965. Mineralogy and sedimentation of recent deep-sea clay in the Atlantic Ocean and adjacent seas and oceans. Geol. Soc. Am. Bull. 76 (7), 803–832.
Chamley, H., 1989. Clay Minerals, Clay Sedimentology. Springer, pp. 3–20.
Chang, F., Li, T., Xiong, Z., Xu, Z., 2015. Evidence for sea level and monsoonally driven variations in terrigenous input to the northern East China Sea during the last 24.3 ka. Paleoceanography 30 (6), 642–658.
Clift, P.D., 2006. Controls on the erosion of Cenozoic Asia and the flux of clastic sediment to the ocean. Earth Planet. Sci. Lett. 241 (3), 571–580.
Clift, P.D., 2016. Assessing effective provenance methods for fluvial sediment in the South China Sea. Geol. Soc. Lond., Spec. Publ. 429 (1), 9–29.
Clift, P.D., Blusztajn, J., 2005. Reorganization of the western Himalayan river system after five million years ago. Nature 438 (7070), 1001–1003.
Clift, P.D., Wan, S., Blusztajn, J., 2014. Reconstructing chemical weathering, physical erosion and monsoon intensity since 25 Ma in the northern South China Sea: a review of competing proxies. Earth Sci. Rev. 130, 86–102.
Colin, C., Turpin, L., Blamart, D., Frank, N., Kissel, C., Duchamp, S., 2006. Evolution of weathering patterns in the Indo-Burman Ranges over the last 280 kyr: effects of sediment provenance on87Sr/86Sr ratios tracer. Geochem. Geophys. Geosyst. 7 (3), Q03007. http://dx.doi.org/10.1029/2005GC000962.
Colin, C., Siani, G., Sicre, M.-A., Liu, Z., 2010. Impact of the East Asian monsoon rainfall changes on the erosion of the Mekong River basin over the past 25,000 yr. Mar. Geol. 271 (1), 84–92.
Cutler, K.B., Edwards, R.L., Taylor, F.W., Cheng, H., Adkins, J., Gallup, C.D., Cutler, P.M., Burr, G.S., Bloom, A.L., 2003. Rapid sea-level fall and deep-ocean temperature change since the last interglacial period. Earth Planet. Sci. Lett. 206 (3), 253–271.
Dane, J., Topp, G., Campbell, G., Horton, R., Jury, W., Nielsen, D., van Es, H., Wierenga, P., Topp, G., 2002. Part 4. Physical Methods. Methods of Soil Analysis. Soil Science Society of America, Madison, WI.
Diekmann, B., Hofmann, J., Henrich, R., Fütterer, D.K., Röhl, U., Wei, K.Y., 2008. Detrital sediment supply in the southern Okinawa Trough and its relation to sea-level and Kuroshio dynamics during the late Quaternary. Mar. Geol. 255 (1–2), 83–95.
Dou, Y., Yang, S., Liu, Z., Clift, P.D., Shi, X., Yu, H., Berne, S., 2010a. Provenance discrimination of siliciclastic sediments in the middle Okinawa Trough since 30 ka: constraints from rare earth element compositions. Mar. Geol. 275 (1–4), 212–220.
Dou, Y., Yang, S., Liu, Z., Clift, P.D., Yu, H., Berne, S., Shi, X., 2010b. Clay mineral evolution in the central Okinawa Trough since 28 ka: implications for sediment provenance and paleoenvironmental change. Palaeogeogr. Palaeoclimatol. Palaeoecol. 288 (1–4), 108–117.
Dou, Y., Yang, S., Shi, X., Clift, P.D., Liu, S., Liu, J., Li, C., Bi, L., Zhao, Y., 2016. Provenance weathering and erosion records in southern Okinawa Trough sediments since 28 ka: geochemical and Sr–Nd–Pb isotopic evidences. Chem. Geol. 425, 93–109.
Dykoski, C.A., Edwards, R.L., Cheng, H., Yuan, D., Cai, Y., Zhang, M., Lin, Y., Qing, J., An, Z., 2005. A high-resolution, absolute-dated Holocene and deglacial Asian monsoon record from Dongge Cave, China. Earth Planet. Sci. Lett. 233 (1), 71–86.
Fedo, C.M., Nesbitt, H.W., Young, G.M., 1995. Unraveling the effects of potassium metasomatism in sedimentary rocks and paleosols, with implications for paleoweathering conditions and provenance. Geology 23 (10), 921–924.
Fralick, P., Kronberg, B., 1997. Geochemical discrimination of clastic sedimentary rock sources. Sediment. Geol. 113 (1), 111–124.
Gaillardet, J., Dupré, B., Allègre, C., 1999. Geochemistry of large river suspended sediments: silicate weathering or recycling tracer? Geochim. Cosmochim. Acta 63 (23), 4037–4051.
Garzanti, E., Padoan, M., Setti, M., López-Galindo, A., Villa, I.M., 2014. Provenance versus weathering control on the composition of tropical river mud (southern Africa). Chem. Geol. 366, 61–74.
Glasby, G.P., Notsu, K., 2003. Submarine hydrothermal mineralization in the Okinawa Trough, SW of Japan: an overview. Ore Geol. Rev. 23 (3–4), 299–339.
Gromet, L.P., Haskin, L.A., Korotev, R.L., Dymek, R.F., 1984. The "North American shale composite": its compilation, major and trace element characteristics. Geochim. Cosmochim. Acta 48 (12), 2469–2482.
Guo, Z., Yang, Z., Lei, K., Gao, L., Qu, Y., 2001. The distribution and composition of suspended matters and their influencing factors in the central-southern area of Okinawa Trough and its adjacent shelf sea. Acta Oceanol. Sin. 1, 008.
Hu, B., Li, G., Li, J., Bi, J., Zhao, J., Bu, R., 2012. Provenance and climate change inferred from Sr-Nd-Pb isotopes of late Quaternary sediments in the Huanghe (Yellow River) Delta, China. Quat. Res. 78 (3), 561–571.
Hu, D., Böning, P., Köhler, C.M., Hillier, S., Pressling, Nicola, Wan, S., Brumsack, H.J., Clift, P.D., 2012. Deep sea records of the continental weathering and erosion response to East Asian monsoon intensification since 14 ka in the South China Sea. Chem. Geol. 326-327, 1–18.
Hu, D., Clift, P.D., Böning, P., Hannigan, R., Hillier, S., Blusztajn, J., Wan, S., Fuller, D.Q., 2013. Holocene evolution in weathering and erosion patterns in the Pearl River delta. Geochem. Geophys. Geosyst. 14 (7), 2349–2368.
Huang, J., Wan, S., Xiong, Z., Zhao, D., Liu, X., Li, A., Li, T., 2016. Geochemical records of Taiwan-sourced sediments in the South China Sea linked to Holocene climate changes. Palaeogeogr. Palaeoclimatol. Palaeoecol. 441, 871–881.
Jones, C.E., Halliday, A.N., Rea, D.K., Owen, R.M., 2000. Eolian inputs of lead to the North Pacific. Geochim. Cosmochim. Acta 64 (8), 1405–1416.
Jones, M.T., Pearce, C.R., Oelkers, E.H., 2012. An experimental study of the interaction of basaltic riverine particulate material and seawater. Geochim. Cosmochim. Acta 77, 108–120.
Ju, L., Wang, H., Jiang, D., 2007. Simulation of the Last Glacial Maximum climate over East Asia with a regional climate model nested in a general circulation model. Palaeogeogr. Palaeoclimatol. Palaeoecol. 248 (3), 376–390.
Kang, L., Wang, J., Liu, H., Wang, Y., Zuo, Z., Chen, J., 2005. Analysis of the historic change on the Lanzhou's runoff from the upper reaches of the Yellow River. J. Hydraul. Eng. 2005, 30–35.
Kasai, M., Marutani, T., Brierley, G.J., 2004. Patterns of sediment slug translation and dispersion following typhoon-induced disturbance, Oyabu Creek, Kyushu, Japan. Earth Surf. Process. Landf. 29 (1), 59–76.

Kawahata, H., Nohara, M., Aoki, K., Minoshima, K., Gupta, L.P., 2006. Biogenic and abiogenic sedimentation in the northern East China Sea in response to sea-level change during the Late Pleistocene. Glob. Planet. Chang. 53 (1), 108–121.
Kubota, Y., Kimoto, K., Tada, R., Oda, H., Yokoyama, Y., Matsuzaki, H., 2010. Variations of East Asian summer monsoon since the last deglaciation based on Mg/Ca and oxygen isotope of planktic foraminifera in the northern East China Sea. Paleoceanography 25 (4), 1971–1982.
Kump, L.R., Brantley, S.L., Arthur, M.A., 2000. Chemical weathering, atmospheric CO_2, and climate. Annu. Rev. Earth Planet. Sci. 28 (1), 611–667.
Lee, S., Kim, J., Yang, D., Kim, J., 2008. Rare earth element geochemistry and Nd isotope composition of stream sediments, south Han River drainage basin, Korea. Quat. Int. 176, 121–134.
Li, T., Chang, F., 2009. Paleoceanography in the Okinawa Trough. Ocean Press, Beijing.
Li, F., Yu, J., Jiang, X., Du, Q., Song, H., 1991. Study on buried paleo-channel system in the South Yellow Sea (in Chinese with English abstract). Oceanol. Et Limnol. Sin. 22 (6), 501–508.
Li, G., Liu, Y., Yang, Z., Yue, S., Yang, W., Han, X., 2005. Ancient Changjiang channel system in the East China Sea continental shelf during the last glaciation. Sci. China Ser. D Earth Sci. 48 (11), 1972–1978.
Li, C., Shi, X., Kao, S.J., Liu, Y., Lyu, H.Z., Liu, S., Qiao, S., 2013. Rare earth elements in fine-grained sediments of major rivers from the high-standing island of Taiwan. J. Asian Earth Sci. 69, 39–47.
Li, T., Xu, Z., Lim, D., Chang, F., Wan, S., Jung, H., Cho, J., 2015. Sr-Nd isotopic constraints on detrital sediment provenance and paleoenvironmental change in the northern Okinawa Trough during the late Quaternary. Palaeogeogr. Palaeoclimatol. Palaeoecol. 430, 74–84.
Limmer, D.R., BöNing, P., Giosan, L., Ponton, C., KöHler, C.M., Cooper, M.J., Tabrez, A.R., Clift, P.D., 2012. Geochemical record of Holocene to recent sedimentation on the Western Indus continental shelf, Arabian Sea. Geochem. Geophys. Geosyst. 13 (1).
Liu, J., Milliman, J., Gao, S., 2001. The Shandong mud wedge and post-glacial sediment accumulation in the Yellow Sea. Geo-Mar. Lett. 21 (4), 212–218.
Liu, J.P., Xue, Z., Ross, K., Yang, Z., Gao, S., 2009. Fate of sediments delivered to the sea by Asian large rivers: long-distance transport and formation of remote alongshore clinothems. Sediment. Theatr. Rec. 7 (1).
Liu, J., Saito, Y., Kong, X., Wang, H., Wen, C., Yang, Z., Nakashima, R., 2010. Delta development and channel incision during marine isotope stages 3 and 2 in the western South Yellow Sea. Mar. Geol. 278 (1), 54–76.
Ludwig, W., Amiotte-Suchet, P., Probst, J.L., 1999. Enhanced chemical weathering of rocks during the last glacial maximum: a sink for atmospheric CO_2? Chem. Geol. 159 (1), 147–161.
Machida, H., 1999. The stratigraphy, chronology and distribution of distal marker-tephras in and around Japan. Glob. Planet. Chang. 21 (1), 71–94.
Milliman, J.D., Farnsworth, K.L., 2011. River Discharge to the Coastal Ocean: A Global Synthesis. Cambridge University Press.
Milliman, J.D., Qin, Y., Park, Y.A., 1989. Sediments and Sedimentary Processes in the Yellow and East China Seas. Sedimentary Facies in the Active Plate Margin. Terra Scientific Publishing Company, Tokyo, pp. 233–249.
Moore, D.M., Reynolds, R.C., 1989. X-ray Diffraction and the Identification and Analysis of Clay Minerals. vol. 378 Oxford university press Oxford.
Nakai, S.i., Halliday, A.N., Rea, D.K., 1993. Provenance of dust in the Pacific Ocean. Earth Planet. Sci. Lett. 119 (1), 143–157.
Nesbitt, H.W., Markovics, G., 1997. Weathering of granodioritic crust, long-term storage of elements in weathering profiles, and petrogenesis of siliciclastic sediments. Geochim. Cosmochim. Acta 61 (8), 1653–1670.
Nesbitt, I., Young, G., 1982. Early Proterozoic climates and plate motions inferred from major element chemistry of lutites. Nature 299, 21.
Nesbitt, H., Young, G.M., 1989. Formation and diagenesis of weathering profiles. J. Geol. 129–147.
Nie, J., Stevens, T., Rittner, M., Stockli, D., Garzanti, E., Limonta, M., Bird, A., Andò, S., Vermeesch, P., Saylor, J., Lu, H., Breecker, D., Hu, X., Liu, S., Resentini, A., Vezzoli, G., Peng, W., Carter, A., Ji, S., Pan, B., 2015. Loess plateau storage of northeastern Tibetan plateau-derived Yellow River sediment. Nat. Commun. 6, 49–55.
Qin, Y., 1996. Geology of the East China Sea. (Science Pr).
Qin, Y., Zhao, Y., Chen, L., Zhao, S., 1989. Geology of the Yellow Sea. Oceanic Publish House, Beijing.
Raymo, M.E., Ruddiman, W.F., Froelich, P.N., 1988. Influence of late Cenozoic mountain building on ocean geochemical cycles. Geology 16 (7), 649–653.
Ren, M., Shi, Y., 1986. Sediment discharge of the Yellow River (China) and its effect on the sedimentation of the Bohai and the Yellow Sea. Cont. Shelf Res. 6 (6), 785–810.
Riebe, C.S., Kirchner, J.W., Finkel, R.C., 2004. Erosional and climatic effects on long-term chemical weathering rates in granitic landscapes spanning diverse climate regimes. Earth Planet. Sci. Lett. 224 (3), 547–562.
Saito, Y., Katayama, H., Ikehara, K., Kato, Y., Matsumoto, E., Oguri, K., Oda, M., Yumoto, M., 1998. Transgressive and highstand systems tracts and post-glacial transgression, the East China Sea. Sediment. Geol. 122 (1), 217–232.
Saito, Y., Wei, H., Zhou, Y., Nishimura, A., Sato, Y., Yokota, S., 2000. Delta progradation and chenier formation in the Huanghe (Yellow River) delta, China. J. Asian Earth Sci. 18 (4), 489–497.
Scholz, F., Hensen, C., Schmidt, M., Geersen, J., 2013. Submarine weathering of silicate minerals and the extent of pore water freshening at active continental margins. Geochim. Cosmochim. Acta 100, 200–216.
Selvaraj, K., Chen, C.T.A., 2006. Moderate chemical weathering of subtropical Taiwan: constraints from solid-phase geochemistry of sediments and sedimentary rocks. J. Geol. 114 (1), 101–116.
Shinjo, R., Woodhead, J.D., Hergt, J.M., 2000. Geochemical variation within the northern Ryukyu Arc: magma source compositions and geodynamic implications. Contrib. Mineral. Petrol. 140 (3), 263–282.
Sidle, R.C., Masahiro, C., 2004. Landslides and debris flows strike Kyushu, Japan. EOS Trans. Am. Geophys. Union 85 (15), 145–151.
Song, Y.-H., Choi, M.S., 2009. REE geochemistry of fine-grained sediments from major rivers around the Yellow Sea. Chem. Geol. 266 (3), 328–342.
Stumm, W., Morgan, J.J., 2012. Aquatic Chemistry: Chemical Equilibria and Rates in Natural Waters. vol. 126 John Wiley & Sons.
Sun, Y., Chen, J., Clemens, S.C., Liu, Q., Ji, J., Tada, R., 2006. East Asian monsoon variability over the last seven glacial cycles recorded by a loess sequence from the northwestern Chinese loess plateau. Geochem. Geophys. Geosyst. 7 (12), 97–112.
Tada, R., Murray, R.W., Alvarez Zarikian, C.A.A., Anderson, W.T.J., Bassetti, M.A., Brace, B.J., Clemens, S.C., Gurgel, M.H., Dickens, G.R., Dunlea, A.G., Gallagher, S.J., Giosan, L., Henderson, A.C.G., Holbourn, A.E., Ikehara, K., Irino, T., Itaki, T., Karasuda, A., Kinsley, C.W., Kubota, Y., Lee, G.S., Lee, K.E., Lofi, J., Lopes, C., Peterson, L.C., Saavedra-Pellitero, M., Sagawa, T., Singh, R.K., Sugisaki, S., Toucanne, S., Wan, S., Xuan, C., Zheng, H., Ziegler, M., 2014. Asian Monsoon: onset and evolution of millennial-scale variability of Asian monsoon and its possible relation with Himalaya and Tibetan Plateau uplift. In: IODP Preliminary Report. vol. 346http://dx.doi.org/10.2204/iodp.pr.346.2014.
Taylor, S.R., McLennan, S.M., 1985. The Continental Crust: Its Composition and Evolution.
Tjallingii, R., Stattegger, K., Wetzel, A., Van Phach, P., 2010. Infilling and flooding of the Mekong River incised valley during deglacial sea-level rise. Quat. Sci. Rev. 29 (11), 1432–1444.
Ujiie, H., Tanaka, Y., Ono, T., 1991. Late Quarternary paleoceanographic record from the middle Ryukyu Trench slope, northwest Pacific. Mar. Micropaleontol. 18 (1), 115–128.
Um, I.K., Choi, M.S., Lee, G.S., Chang, T.S., 2015. Origin and depositional environment of fine-grained sediments since the last glacial maximum in the southeastern Yellow Sea: evidence from rare earth elements. Geo-Mar. Lett. 35 (6), 421–431.
Wan, S., Li, A., Clift, P.D., Stuut, J.-B.W., 2007. Development of the East Asian monsoon: mineralogical and sedimentologic records in the northern South China Sea since 20 Ma. Palaeogeogr. Palaeoclimatol. Palaeoecol. 254 (3), 561–582.
Wan, S., Clift, P.D., Li, A., Li, T., Yin, X., 2010. Geochemical records in the South China Sea: implications for East Asian summer monsoon evolution over the last 20 Ma. Geol. Soc. Lond., Spec. Publ. 342 (1), 245–263.
Wan, S., Clift, P.D., Li, A., Yu, Z., Li, T., Hu, D., 2012. Tectonic and climatic controls on long-term silicate weathering in Asia since 5 Ma. Geophys. Res. Lett. 39 (15).
Wan, S., Toucanne, S., Clift, P.D., Zhao, D., Bayon, G., Yu, Z., Cai, G., Yin, X., Revillon, S., Wang, D., Li, A., Li, T., 2015. Human impact overwhelms long-term climate control of weathering and erosion in southwest China. Geology 43 (5), 439–442.
Wan, S., Clift, P.D., Zhao, D., Hovius, N., Munhoven, G., France-Lanord, C., Wang, Y., Xiong, Z., Huang, J., Yu, Z., Zhang, J., Ma, W., Zhang, G., Li, A., Li, T., 2017. Enhanced silicate weathering of tropical shelf sediments exposed during glacial lowstands: a sink for atmospheric CO_2. Geochim. Cosmochim. Acta 200, 123–144.
Wang, Y., Cheng, H., Edwards, R.L., An, Z., Wu, J., Shen, C., Dorale, J.A., 2001. A high-resolution absolute-dated late Pleistocene Monsoon record from Hulu Cave, China. Science 294 (5550), 2345–2348.
Wang, P., Tian, J., Cheng, X., Liu, C., Xu, J., 2003. Carbon reservoir changes preceded major ice-sheet expansion at the mid-Brunhes event. Geology 31 (3), 239–242.
Wang, S., Li, L., Yan, M., 2013. The contributions of climate change and human activities to the runoff yield changes in the middle Yellow River Basin. Geogr. Res. 32 (3), 395–402.
Wang, J., Li, A., Xu, K., Zheng, X., Huang, J., 2015. Clay mineral and grain size studies of sediment provenances and paleoenvironment evolution in the middle Okinawa Trough since 17 ka. Mar. Geol. 366, 49–61.
Wei, G., Liu, Y., Li, X.-h., Shao, L., Fang, D., 2004. Major and trace element variations of the sediments at ODP Site 1144, South China Sea, during the last 230 ka and their paleoclimate implications. Palaeogeogr. Palaeoclimatol. Palaeoecol. 212 (3), 331–342.
West, A.J., 2012. Thickness of the chemical weathering zone and implications for erosional and climatic drivers of weathering and for carbon-cycle feedbacks. Geology 40 (9), 811–814.
West, A.J., Galy, A., Bickle, M., 2005. Tectonic and climatic controls on silicate weathering. Earth Planet. Sci. Lett. 235 (1), 211–228.
Xu, F., Li, A., Li, T., Xu, K., Chen, S., Qiu, L., Cao, Y., 2011. Rare earth element geochemistry in the inner shelf of the East China Sea and its implication to sediment provenances. J. Rare Earths 29 (7), 702–709.
Xu, Z., Li, T., Chang, F., Wan, S., Cho, J., Limc, D., 2014. Clay-sized sediment provenance change in the northern Okinawa Trough since 22 kyrBP and its paleoenvironmental implication. Palaeogeogr. Palaeoclimatol. Palaeoecol. 399, 236–245.
Yan, M., Chi, Q., 2005. The Chemical Compositions of the Continental Crust and Rocks in the Eastern Part of China. Science Press.
Yang, S., Youn, J.S., 2007. Geochemical compositions and provenance discrimination of the central south yellow sea sediments. Mar. Geol. 243 (1), 229–241.
Yang, S., Jung, H., Choi, M., Li, C., 2002. The rare earth element compositions of the Changjiang (Yangtze) and Huanghe (Yellow) river sediments. Earth Planet. Sci. Lett. 201 (2), 407–419.
Yang, S., Jung, H.-S., Li, C., 2004a. Two unique weathering regimes in the Changjiang and Huanghe drainage basins: geochemical evidence from river sediments. Sediment. Geol. 164 (1), 19–34.
Yang, S., Lim, D., Jung, H., Oh, B., 2004b. Geochemical composition and provenance discrimination of coastal sediments around Cheju Island in the southeastern Yellow Sea. Mar. Geol. 206 (1), 41–53.
Yuan, D., Zhu, J., Li, C., Hu, D., 2008. Cross-shelf circulation in the Yellow and East China

Seas indicated by MODIS satellite observations. J. Mar. Syst. 70 (1), 134–149.
Zhang, C., Mischke, S., 2009. A Lateglacial and Holocene lake record from the Nianbaoyeze Mountains and inferences of lake, glacier and climate evolution on the eastern Tibetan Plateau. Quat. Sci. Rev. 28 (19), 1970–1983.
Zhang, J., Huang, W.W., Liu, M.G., Zhou, Q., 1990. Drainage basin weathering and major element transport of two large Chinese rivers (Huanghe and Changjiang). J. Geophys. Res. Oceans 95 (C8), 13277–13288.
Zhao, D., Wan, S., Toucanne, S., Clift, P.D., Tada, R., Révillon, S., Kubota, Y., Zheng, X., Yu, Z., Huang, J., Jiang, H., Xu, Z., Shi, X., Li, A., 2017. Distinct control mechanism of fine-grained sediments from yellow river and Kyushu supply in the northern Okinawa trough since the last glacial. Geochem. Geophys. Geosyst. http://dx.doi.org/10.1002/2016GC006764.
Zheng, X., Li, A., Kao, S.J., Gong, X., Frank, M., Kuhn, G., Cai, W., Yan, H., Wan, S., Zhang, H., Jiang, F., Hathorne, E., Chen, Z., Hu, B., 2016. Synchronicity of Kuroshio Current and climate system variability since the Last Glacial Maximum. Earth Planet. Sci. Lett. 452, 247–257.